Supramolecular Polymers Containing Terpyridine−Metal Complexes in the Side Chain

Khaled A. Aamer[†] and Gregory N. Tew*

Department of Polymer Science and Engineering, University of Massachusetts, Amherst, 120 Governors Drive, Amherst, Massachusetts 01003

Received December 1, 2006; Revised Manuscript Received February 6, 2007

ABSTRACT: The synthesis of supramolecular polymers containing metal complexes in the side chain is described. Atom transfer radical polymerization (ATRP) was used to synthesize the macromolecular backbone, and the metal complex was attached via postpolymerization chemistry. Homopolymers containing $[Ru(terpy)_2]^{2+}$ in the side chain were prepared in which the complex contained either a long hydrophobic C_{16} alkyl group or only hydrogen at the 4′-position. The homopolymers containing the long C_{16} alkyl groups showed lyotropic liquid crystalline (LC) behavior in chloroform solutions from room temperature to 60 °C and self-assembled in the bulk to form hexagonal arrays of cylinders. In addition, this alkyl side chain was observed to crystallize in the solid state. Homopolymers without the C_{16} alkyl group showed no lyotropic LC or any crystallization behavior. The material design emphasizes the relationship between the molecular structure and supramolecular organization of these polymers. It demonstrates that terpy complexes remain a versatile functionality for constructing supramolecular assemblies.

Introduction

Learning to program molecules for self-assembly remains a significant challenge.[1] Despite the great successes discovered over the past two decades, many of the rules for organizing even small molecules are still missing.[2] An even greater challenge is building macromolecules that contain "supramolecular chemistry functional units" and understanding the manifestation of these functional units on the macromolecule's self-assembly. Combining the precision of modern organic polymer chemistry with the rich functionality of metal ions appears to be an extremely fertile area of research.[3] The incorporation of metal ions into polymeric architectures has resulted in an array of novel materials.[4−11]

The greatest majority of these structures have the metal or metal complex in the main chain or at the chain terminus.[12−23] For example, Fraser prepared linear and star polymers with the metal complex at the center as well as multiarm star homo- and diblock copolymers constructed with $[Fe(bpy)_3]^{2+}$ and $[Ru(bpy)_3]^{2+}$ cores.[24,25] In contrast, we and a few others have focused on macromolecular architectures in which the metal complexes are confined to the side chain. Sleiman has explored homopolymers and block copolymers based on oxynorbornenes bearing $[Ru(bpy)_3]^{2+}$ complexes as pendant groups via ring-opening metathesis polymerization (ROMP)[26,27] while Weck prepared diblock and random copolymers based on norbornenes possessing both palladated pincer complexes and diaminopyridine moieties (hydrogen-bonding entities). Noncovalent functionalization in terms of metal complexation and hydrogen bonding was achieved via directed self-assembly, multistep self-assembly, and one-step orthogonal self-assembly with both *N*-butylthymine and pyridine units.[28−31] We are specifically interested in macromolecules containing a dense array of metal complexes along the backbone and how this influences the overall self-assembling properties of the system.

Initially, traditional free radical polymerization was used to prepare supramolecular graft copolymers with functionalized poly(methyl methacrylate) containing terpyridine (terpy) in the side chain.[32] We showed that the addition of Cu^{2+} ions caused an increase in viscosity due to cross-linking while Schubert and co-workers attached poly(ethylene glycol) and polylactide grafts through $[Ru(terpy)_2]^{2+}$ complexes.[33,34] Their graft copolymers with PEG side chains formed micelles in water which were characterized to have high polydispersity in terms of size distribution. The large size distribution was attributed to the high polydispersity of both the polymer backbone and the PEG grafted chains. In order to realize highly ordered materials, better control over the polymer backbone was desired, and we have explored a variety of synthetic approaches to prepare these macromolecules including the use of atom transfer radical polymerization (ATRP), reversible addition−fragmentation chain transfer radical polymerization (RAFT), and nitroxide-mediated radical polymerization (NMP).[35−38]

While great effort has been spent synthesizing these novel macromolecules with metal−ligands at precise locations, in general, studies focused on the self-assembly of metal−ligand side chain polymers has been quite limited. Some reports have described assembly in solution, but very few have examined the solid-state order. Some notable exceptions are the polyelectrolyte, hydrogen-bonded, and metal coordination bottle brush polymers studied by Ikkala and ten Brinke.[39,40] These materials, which take advantage of the pyridine ring in the poly(vinylpyridine) block, are not side-chain-containing metal−ligand polymers per say but use supramolecular interactions to self-assemble macromolecules into a variety of ordered structures including "order-*within*-order" in which structures have lamellae-within-cylinders or cylinders-*within*-lamellae morphology. These materials demonstrated novel properties including lyotropic mesomorphic states and a plethora of hierarchically self-assembled morphologies upon complexation.[41,42]

In this paper, we report novel homopolymers bearing terpy metal complexes on every monomer. We examine their self-assembly into ordered materials in solution and in the solid state. Using ATRP and postfunctionalization to install the $[Ru(terpy)_2]^{2+}$ complex, well-defined polymers up to 470 kDa with

* Corresponding author. E-mail: tew@mail.pse.umass.edu.
[†] Current address: Biomaterials Group, Polymer Division, NIST, 100 Bureau Dr. Stop 8543, Gaithersburg, MD 20899-8543.

10.1021/ma062765i CCC: $37.00 © 2007 American Chemical Society
Published on Web 03/22/2007

Scheme 1. Synthesis of Amine-Functionalized $[Ru(terpy)_2]^{2+}$ Complexes 3 and 4

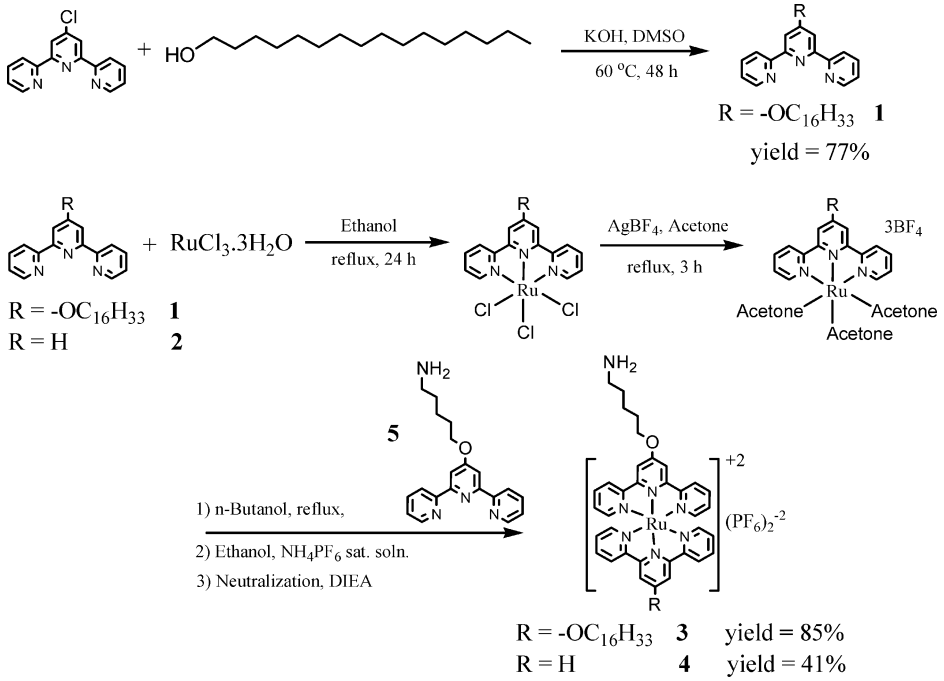

polydispersity of 1.1 were obtained. When the $[Ru(terpy)_2]^{2+}$ complex contains an alkyl tail, the materials from a lyotropic liquid crystalline (LC) phase in chloroform at only 10 wt % and self-assemble with hexagonal order in the solid state. In an effort to understand the importance of the molecular components on this self-organizing behavior, other macromolecules were prepared in which the alkyl chain was removed. These studies demonstrated that it is the combination of all three components—the macromolecular chain, the $[Ru(terpy)_2]^{2+}$ complex, and the alkyl chain—that collectively are responsible for the observed self-assembly.

Results and Discussion

Synthetic Strategy. Discovering new supramolecular materials constructed from macromolecules requires that they be built with a high degree of fidelity over their structure and composition. Polymerizing metal-functionalized monomer directly gives polymers which are hard to characterize using GPC due to adsorption to the column packing materials. There does not appear to be any inherent problem with directly polymerizing the metal functionalized monomer. However, the routine characterization by GPC is extremely difficult, if not impossible. The indirect approach, which involves postpolymerization attachment of the metal complex, has proven to be a much more valuable approach than any direct methods we have discovered to date.[32,35] We reported an indirect approach based on activated esters of *N*-succinimide methacrylate (OSu),[36,38] but here an alternative method is described based on the postfunctionalization of poly(acrylic acid) that uses high yielding peptide chemistries to avoid the possible hydrolysis of the activated esters. In this report, amine-functionalized $[Ru(terpy)_2]^{2+}$ complexes are used to equip the polymer backbone with these supramolecular functionalities in order to determine their influence on the self-assembling behavior of the macromolecular backbone.

Scheme 1 illustrates the synthesis of two different amine-functionalized $[Ru(terpy)_2]^{2+}$ complexes, **3** and **4**, which were covalently attached to the macromolecular backbone. Complex **3** contains a C_{16} alkyl group while complex **4** lacks such a group. These two complexes allowed us to determine the influence of the alkyl group and Ru(II) complex on supramolecular organization independently. Synthesis involves the formation of the single terpy metal complex [Ru(R-terpy)Cl_3], where R is O−$C_{16}H_{33}$ or H, followed by complexation with a second amine-functionalized terpy molecule, **5**. The amine group is used for subsequent coupling to the macromolecular backbone via peptide chemistry, as outlined in Scheme 2.

Synthesis of the macromolecular backbone starts with the polymerization of *tert*-butyl acrylate, P(tBA), using ATRP, followed by deprotection of the *tert*-butyl group to produce poly(acrylic acid), as shown in Scheme 2.[43,44] The metal complexes, **3** or **4**, are reacted with the carboxylic acids on the polymer to give PHBTA and PBTA homopolymers, respectively. This strategy allows us to synthesize the polymer backbone, P(tBA), and characterize it using standard GPC and NMR methods, followed by deprotection and introduction of the amine-functionalized ruthenium complex through standard peptide chemistry, which is known for its very high yield. The design of PHBTA homopolymers includes three different elements, which are crucial in understanding the polymer's self-assembly properties. These elements include a long alkyl C_{16} chain representing a source of hydrophobic interactions and a region suitable for crystallization, an acrylamide polymer backbone which is hydrophilic in nature, and the $[Ru(terpy)_2]^{2+}$ complex with two positive charges which contributes an ionic character to the polymer. As will be described, all three of these distinct components appear to be important for the observed self-assembly of the polymers.

FT-IR Analysis. The largest single concern of the postfunctionalization approach is the extent of reaction on the polymer backbone. Carefully examining the ^{1}H NMR and IR spectra confirmed the ester deprotection and amide bond formation proceeds in very high, ∼99%, yield. On the basis of the characterization of the P(tBA) prepolymer and conversion to the metal complexes, Table 1 provides the molecular weight, degree of polymerization ($\overline{DP}$), and polydispersity index (PDI) for the three polymers containing metal complexes in their side chains that are investigated in this paper.

Scheme 2. Synthesis of PHBTA and PBTA Homopolymers Containing $[Ru(terpy)_2]^{2+}$ Complexes

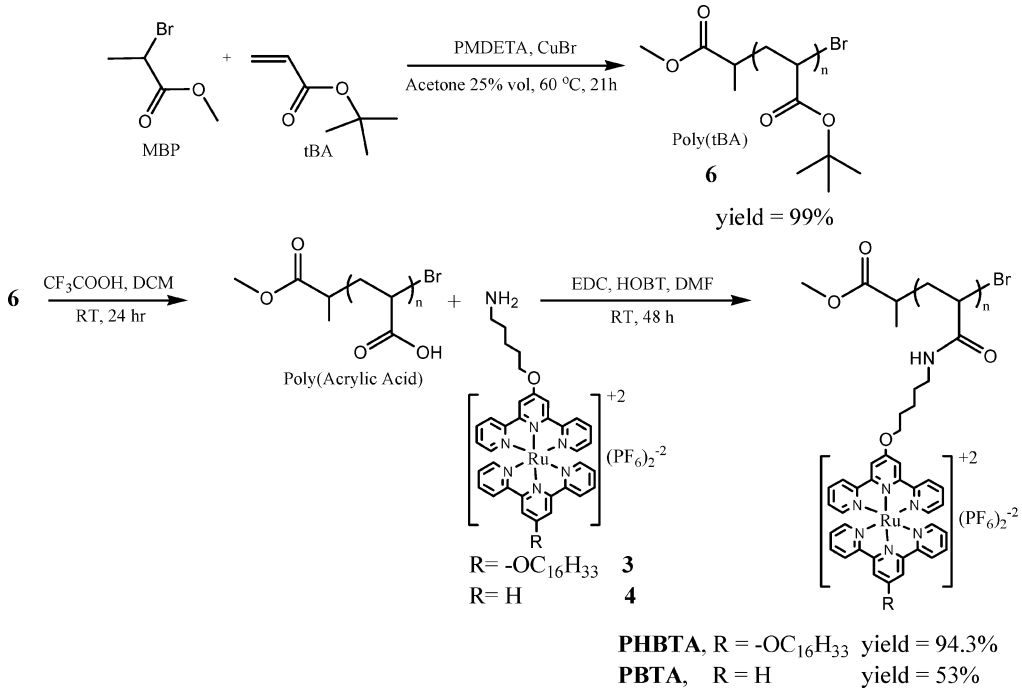

Table 1. Molecular Weight Characterization of PHBTA and PBTA Homopolymers

polymer	M_n[a] × 10^3	$\overline{DP}$[b]	PDI[b]
PHBTA-1	470.0	375	1.12
PHBTA-2	72.7	58	1.11
PBTA	58.7	375	1.12

[a] M_n values are calculated using monomer M_w and $\overline{DP}$ of P(tBA) from GPC measurements. [b] $\overline{DP}$ and PDI are based on the P(tBA**)** protected polymer M_n by THF GPC vs PMMA linear standards and ^{1}H NMR data. Neither deprotection nor coupling affects the carbon backbone of the polymer.

FT-IR is a valuable technique to monitor postfunctionalization, especially in this case due to the changes which occur in the carbonyl functionality. Figure 1 shows the carbonyl region as the *tert*-butyl esters are converted to carboxylic acids and as these carboxylic acids are converted to amides upon attachment of the metal complex. In Figure 1a, the carbonyl stretching vibration corresponding to the *tert*-butyl ester on P(tBA) is shown at $\nu = 1728$ cm^{-1}. After treating P(tBA**)** with TFA, the product's carbonyl stretch shifted to lower wavenumbers at $\nu = 1708$ cm^{-1}. This lower wavenumber vibration appears in the region for poly(acrylic acid) standards and is consistent with the conversion of the *tert*-butyl ester to carboxylic acids. Although the carbonyl band for poly(acrylic acid) is broad and does not shift completely away from 1728 cm^{-1}, ^{1}H NMR spectra show the complete disappearance of the signals corresponding to *tert*-butyl protons. Moreover, further conversion of the sample by incorporating the metal complexes shifts the carbonyl stretching vibration to even lower wavenumbers at $\nu = 1616$ cm^{-1}. This new shift, which is consistent with amide bond formation, moves the vibrational signal far enough that there is essentially no overlap with $\nu = 1728$ cm^{-1}, enabling the region that originally corresponded to the *tert*-butyl ester to be clearly seen. It shows no residual signal consistent with ~99% conversion of the *tert*-butyl esters to the carboxylic acids. Similarly, there appears to be no signal remaining at 1708 cm^{-1} for the carboxylic acid function, suggesting high conversion to the amide. Further examination of the 2500−4000 cm^{-1} region (not shown) shows no signal for the carboxylic acid OH between $\nu = 3100-3500$ cm^{-1} after conversion to the amide. As a result, FT-IR and ^{1}H NMR support ~99% conversion of the prepolymer to the metal complex containing polymers PHBTA or PBTA.

Optical Properties. Absorption spectra of complex **3** and homopolymer PHBTA were obtained at room temperature in acetonitrile, as shown in Figure 2.

The spectra show normalized absorption bands in the UV region, which are attributed to the terpy electronic transitions and in the visible region associated with the dπ (Ru)−π*(terpy) metal-to-ligand charge-transfer (MLCT) band.[45] The UV/vis spectra of complex **3** and homopolymer PHBTA look very similar, which is an indication that the attachment of complex **3** to the macromolecular backbone has very little, if any, effect on their absorption properties. The molar absorptivity data in Table 2 show the close ϵ values between complex **3** and the corresponding polymers at the four peak maxima. This comparison of ϵ between **3** and the PHBTA polymers provides two important pieces of information. First, it confirms the high conversion of the amide coupling reaction. If the number of metal complexes along the backbone where much less than ~100%, then the determination of the molar absorptivity between **3** and the macromolecules containing **3** in the side chain would show deviation. Second, a comparison between PHBTA-**1** and PHBTA-**2** shows that $\overline{DP}$ has very little effect on ϵ. As a result, the PHBTA polymers can be visualized as a number of independent chromophores attached to the polymer backbone, in agreement with observations from Sleiman on ROMP polymers with $[Ru(bpy)_3](PF_6)_2$ attached to the side chain via ethylene glycol linkers.[26] Similar observations were found for the PBTA polymer and complex **4**. $[Ru(terpy)_2]^{2+}$ complexes show very weak emission compared to most ruthenium(II)−polypyridine complexes. This observation is attributed to the equilibration of the ^{3}MLCT state with high-spin d−d (metal centered, MC) states. The depopulation of the ^{3}MLCT by the low-lying MC state is a direct result of the unfavorable bite angles associated with the terpy ligand which causes deviation from the idealized octahedral geometry. Because the $[Ru(terpy)_2](PF_6)_2$ complex has very weak emission at room temperature,[36]

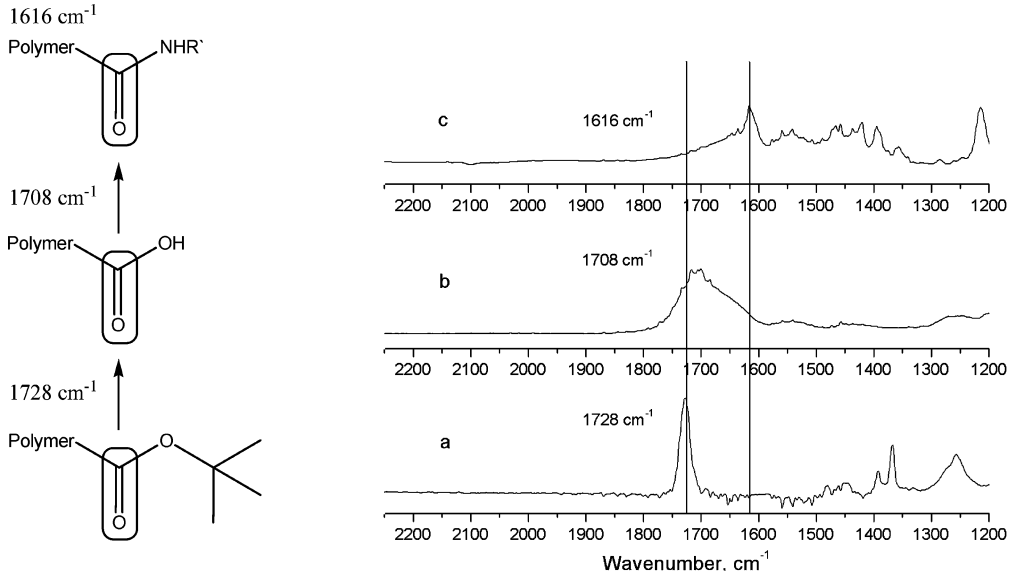

Figure 1. FTIR stacked spectra of (a) PtBA, (b) poly(acrylic acid), and (c) PHBTA homopolymers in the range 2250−1200 cm^{-1}.

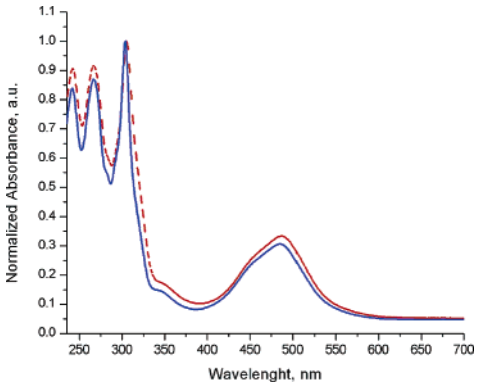

Figure 2. UV/vis overlaid spectra of complex **3** (solid line) and PHBTA (broken line) homopolymer.

we did not record emission spectra for the complex **3** or the PHBTA homopolymers, and as a result, our conclusions regarding the effect of the polymer backbone on the electronic properties of $[Ru(terpy)_2]^{2+}$ covers only the absorption properties or their ground state interactions.

Supramolecular Organization. Lyotropic Liquid Crystal Properties. Having successfully prepared and characterized these macromolecules, their ability to self-assemble into ordered materials was first examined in solution. Figure 3 shows the polarized optical microscopy (POM) image of a 15 wt % PHBTA-1 solution in chloroform. The image shows red bright areas aligned in the direction of shear, indicating a liquid crystalline (LC) phase that remains present upon heating from room temperature to about 60 °C (the boiling point of chloroform). For PHBTA-1 with $\overline{DP} = 375$, birefringence in chloroform solution was observed down to 8 wt %. To better understand the molecular origin of this LC solution, two different molecules were investigated. Initially, the effect of the molecular weight (MW) was examined using PHBTA-2 which has a $\overline{DP} = 58$ compared to $\overline{DP} = 375$ for PHBTA-1.

Like PHBTA-1, PHBTA-2 is birefringent in chloroform at 15 wt %, but when the concentration is reduced below 10 wt %, the birefringence is lost. These data show that the shorter polymer (4.6 times smaller $\overline{DP}$) requires a 2 wt % higher concentration to exhibit birefringence and thus long-range order. This slight increase in concentration, from 8 wt % for PHBTA-1 to 10 wt % for the shorter PHBTA-2, shows that MW does not have a significant influence on the lyotropic behavior of these polymers. This slight decrease from 10 to 8 wt % is consistent with the expectation that the smaller MW sample requires slightly more material in solution to experience intermolecular interactions leading to long-range order. Next, the influence of the C_{16} alkyl side chain was examined with PBTA in acetone since it is not soluble in chloroform. This material demonstrated no lyotropic phase behavior at any concentration up to 20 wt %, suggesting the presence of the metal complex alone is not enough to drive assembly in solution. It suggests the C_{16} chain plays an important role in stiffening the macromolecular backbone and promoting attractive interactions between chains which leads to self-organization. At the same time, it seemed unreasonable to conclude that the metal complex plays no role in the organization since poly(acrylamide)s with long alkyl side chains are not typically known to be lyotropic in organic solvents.[52]

Speculating that the metal complex has ionic character, we performed a classical polyelectrolyte experiment in which the reduced viscosity of PBTA was measured as a function of polymer concentration. As a result of the electroviscous effect, conventional polyelectrolytes show an increase in viscosity as the concentration is reduced.[46,47] This increase in viscosity with decreasing concentration results from an expansion of the macromolecular chain as the effective salt concentration is lowered due to the reduced number of polyelectrolyte counterions in solution. Figure 4 shows that the reduced viscosity as a function of polymer concentration gradually increases with decreasing polymer concentration for PBTA. This data supports the assumption that the metal complex is ionized enough that the electrostatic interactions along the polymer backbone are manifested in the dilute regime, leading to an expansion of the polymer chain and subsequent increase in solution viscosity. In addition to this electroviscous effect, PBTA solutions show conductance demonstrating the presence of free ions and the dissociation of the counterions from the metal complex. These experiments demonstrate the metal complex behaves as a charged group within the polymer backbone.

Since the metal complex has a charged nature and the C_{16} alkyl chain is necessary to exhibit lyotropic materials, similarities between these novel polymers and polyelectrolyte−surfactant complexes become apparent. Figure 5 shows a structural comparison between the PHBTA polymers and a polyelectro-

Table 2. Molar Absorptivity Data for Complex 3, PHBTA-1, and PHBTA-2

	ϵ (M^{-1} cm^{-1} × 10^4)[a]			
compound	λ_{max} = 242 nm	λ_{max} = 267 nm	λ_{max} = 304 nm	λ_{max} = 484 nm
complex **3**	4.72	4.82	5.64	1.61
PHBTA-1, $\overline{DP}$ = 375	4.57	4.76	5.25	1.62
PHBTA-2, $\overline{DP}$ = 58	4.52	4.78	5.28	1.62

[a] ϵ units are reported per mole of the monomer containing $[Ru(terpy)_2]^{2+}$ complex.

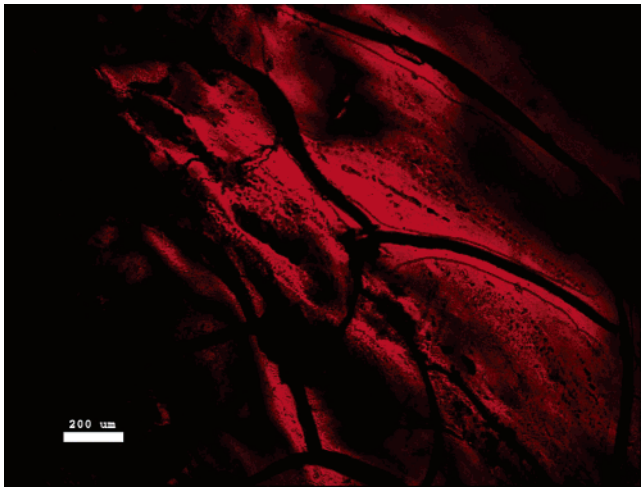

Figure 3. Polarized optical microscopy micrograph of PHBTA-1, 15 wt %, in chloroform at room temperature sheared by sliding the coverslip.

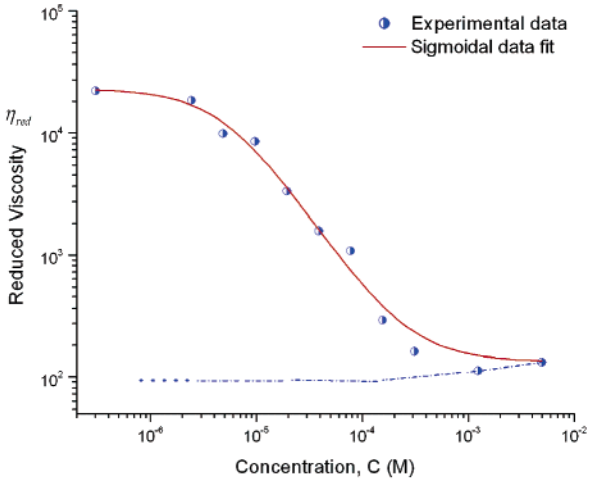

Figure 4. Reduced viscosity measured as a function of monomer concentration for PBTA in acetonitrile at 22 °C. Circular points are the experimental data, the solid line is a sigmoidal fit, and the dotted line is a theoretical behavior expected for a noncharged polymer.

lyte−surfactant complex. In each system, the side chain contains a charged group ($[Ru(terpy)_2]^{2+}$ metal complex or SO_3^-) and long alkyl chain. This creates another level of structural segregation within the macromolecule since the alkyl chain is hydrophobic and the charged group is more polar.

In order to further understand the self-assembly of these metal−ligand containing polymers, we turned to the theoretical analysis which describes the stiffening of flexible, linear polyelectrolyte chains due to complexation with oligomeric surfactants by Frederickson.[48] These interactions induce lyotropic LC behavior in solution, even for very flexible polymers. According to the theory, flexible polymers bound to surfactants will, under good solvent conditions for the alkyl chain, develop sufficient enhancement of the persistence length due to steric interactions originating from the excluded-volume repulsion

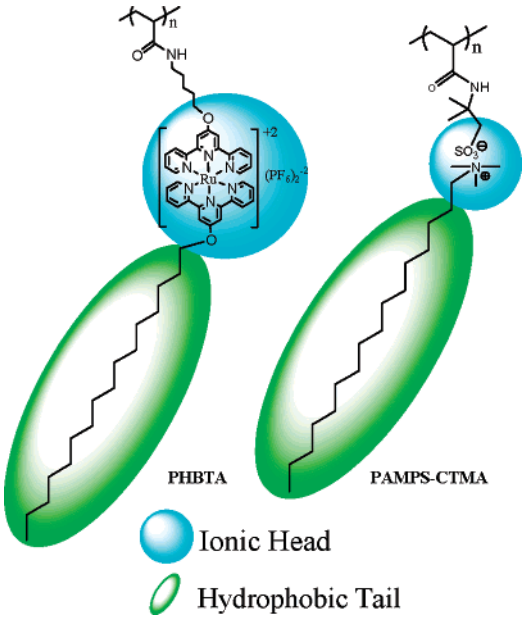

Figure 5. Structural analogy between PHBTA and poly(2-acrylamido-2-methyl-1-propanesulfonate cetyltrimethylammonium salt), PAMPS−CTMA. Each structure is composed from an acrylamide backbone with side chains containing a charge unit and long hydrophobic alkyl group.

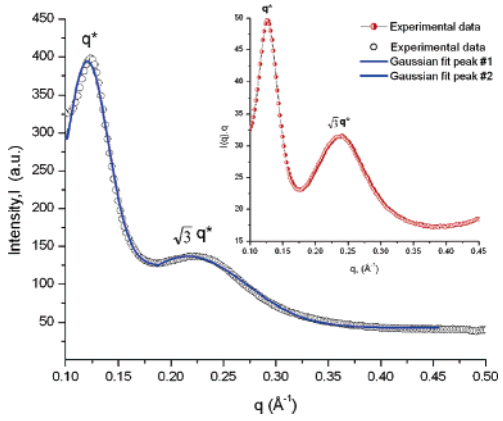

Figure 6. SAXS pattern for PHBTA-1: open circles, observed data set; solid line, curve fitting to a Gaussian distribution. Inset: $I(q)q$ vs q presentation of the same data set for better recognition of the higher order peak.

between alkyl chains. Essential parameters are the number of binding sites, the binding energies, and the length of the alkyl chain surfactant M. For a given M, the number of bound alkyl chains per monomer, σ, determines the stiffness of the complex. At the high coverage limit, the persistence length λ of the complex is predicted to scale to M according to eq 1[39,48]

$$\lambda \propto a\sigma^{17/8}M^{15/8} \quad (1)$$

where a is the Kuhn segment size (for simplicity, it is assumed to be the same for the polymer and surfactant). The thickness

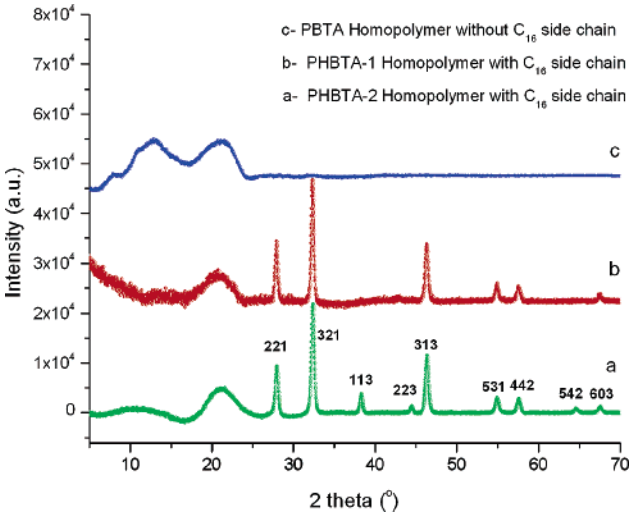

Figure 7. Wide-angle powder X-ray diffraction pattern of (a) PHBTA-2, (b) PHBTA-1, and (c) PBTA homopolymers.

Table 3. Unit Cell Parameters and Lattice Type for PHBTA-2 Homopolymer

polymer	unit cell parameters	crystal lattice type	$\langle L \rangle_{vol}$, nm
PHBTA-2, $\overline{DP} = 58$	$a = b =$ 10.0278 Å	tetragonal, P type	17.7 for (531)
	$c = 7.5070$ Å		21.8 for (542)
	$\alpha = \beta = \delta = 90°$		

of the polymer−surfactant complex R is predicted to scale according to eq 2.[48]

$$R \propto a\sigma^{1/4}M^{3/4} \tag{2}$$

As a consequence, the ratio λ/R, which determines the possibility of lyotropic behavior, scales according to eq 3.[48]

$$\lambda/R \propto \sigma^{15/8}M^{9/8} \tag{3}$$

In order to observe lyotropic behavior, this ratio should exceed 10,[48,49] which taken at face value would also require the side chains to consist of ~10 methylene units ($M = 10$) provided that every monomer repeat unit contains an alkyl chain as is the case for our PHBTA polymers, (i.e., $\sigma \cong 1$).[39,50]

Specifically in our PHBTA polymers, the metal−ligand complex forces every monomer unit to have an alkyl tail which turns the flexible poly(acrylic acid) backbone into a rigid-rod-like chain. The rigidity is a result of stiffening the polymer backbone due to the excluded-volume repulsion of the C_{16} alkyl groups and the $[Ru(terpy)_2]^{2+}$ complex. Since PBTA and noncharged polyacrylamides containing long alkyl groups do not show lyotropic LC behavior, it suggests that the $[Ru(terpy)_2]^{2+}$ complex and C_{16} alkyl chain are necessary to induce lyotropic LC properties in PHBTA.[51,52]

Solid-State Assembly. Having characterized the solution behavior of these polymers, their solid-state organization was examined by SAXS and WAXD. The lyotropic LC properties suggested the PHBTA polymers acted like rigid rods in solution. If this were the case, they may self-organize into ordered materials in the solid state. POM experiments first indicated these materials were ordered in the solid state due to the presence of birefringence textures from solid samples. In contrast, PBTA showed no birefringence in the solid state.

SAXS experiments were performed on samples of PHBTA-1 cast from the 15 wt % chloroform lyotropic LC solution, and the obtained scattering pattern is shown in Figure 6. From the

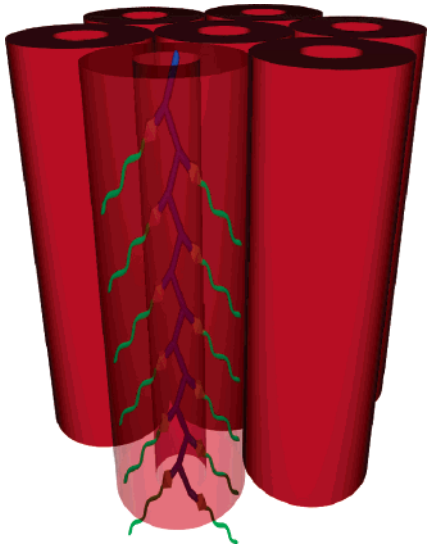

Figure 8. Schematic representation showing the hexagonal array of cylinders. The macromolecule is shown superimposed on one of the cylinders. The cylinders are not hollow but represent the amorphous nature of the backbone and $[Ru(terpy)_2]^{2+}$ while the solid red represents the crystalline alkyl chains.

$1:\sqrt{3}$ ratio, a model was developed on the basis of a hexagonal array of cylinders with a lattice spacing of 5.1 nm. This model was initially developed on the basis of the observed lyotropic LC phase and previous studies on "hairy" rod polymers with high persistence length. According to Ikkala and ten Brinke,[49] rigid-rod polymers show three possible microphase-separated morphologies including one which is lamellae and two which are hexagonal. The lamellar phases are observed with short side chains while long side chains promote hexagonal ordering of the hairy-rod cylindrical brushes. In the intermediate length side chain regime, several chains associate to form elongated cylinders. Fitting the measured q spacings to our macromolecular structure with consideration of these phases, we arrived at a hexagonal array in which the side chains are tilted about 45° with respect to the molecular backbone. Assuming close packing of the cylinders, along with the calculated molecular dimensions from molecular modeling in which the fully extended side chain is 4.2 nm, the cylinder diameter with fully extended chains would be 8.4 nm. Allowing the side chains to tilt ~45° provides a cylinder diameter of $d_c = 5.89$ nm and an excellent match for the observed lattice spacing of 5.1 nm. This tilt angle of 45° is similar to commonly observed tilt angles of mesogen-jacketed liquid crystalline polymers in which the tilt angle is about 38°.[53]

At the same time, alkyl side chains containing 16 carbon atoms are known to crystallize. WAXD experiments were performed and showed crystalline diffraction peaks for PHBTA-1 and 2, which were absent in PBTA (see Figure 7). This clearly indicates that the C_{16} alkyl chain is responsible for the sharp peaks observed in Figure 7. Fitting the sharp signals provided unit cell parameters and the crystal lattice type, which are summarized in Table 3. Both PHBTA-1 and 2 polymers were fit to the same unit cell although PHBTA-2 has three signals for (113), (223), and (542) planes, which are very weak or absent in PHBTA-1. The polymer crystallite size, $\langle L \rangle_{vol}$, was calculated from the Scherrer equation,[39] using the crystalline diffraction signals for both PHBTA polymers and ranged from 17.7 to 21.8 nm. The broad signals shown between $2\theta = 10-25°$ correspond to amorphous scattering of the polymer backbone and that part of the side chains which are not crystalline (the C_5 segment between the backbone and the $[Ru(terpy)_2]^{2+}$

complex). Examination of the scattering data obtained from PBTA shows the lack of crystalline scattering but the continued presence of the amorphous scattering due to the polymer backbone.

Figure 8 shows a representation of the supramolecular assembly generated from the diffraction data just presented. The lyotropic LC properties initially suggested that the PHBTA polymers behaved like rigid rods. The SAXS pattern showed a hexagonal lattice whose dimensions were consistent with the chemical structure of PHBTA. The side chains tilt away from the molecular backbone at an angle of about 45°, which is consistent with typical observations seen for mesogen-jacketed liquid crystalline polymers.[53] WAXD indicated the long alkyl chains actually crystallize within the supramolecular assembly, providing a strong driving force for macromolecular self-assembly.

Figure 8 illustrates the hexagonal array of cylinders as well as the fact that the alkyl chain crystallize while the $[Ru(terpy)_2]^{2+}$ and the polymer are amorphous.

Conclusions

The synthesis of novel $[Ru(terpy)_2]^{2+}$ complex containing polymers was accomplished using ATRP followed by postpolymerization functionalization. When the macromolecular architecture included both the metal complex and alkyl chain, self-assembly was observed in solution and in the solid state. Because the metal complex was shown to be charged, structural analogy to polyelectrolyte−surfactant complexes could be made, which helped in understanding the noncovalent forces guiding self-assembly. Polymers containing $[Ru(terpy)_2]^{2+}$ complexes in the side chain could find potential applications in constructing multicomponent systems for photoinduced charge separation. Polymers provide several handles for tuning properties including the polymer molecular weight, architecture, composition, and self-assembling properties. The impact of incorporating $[Ru(terpy)_2]^{2+}$ complexes on the properties of these polymers is well illustrated by the electroviscous effect, the ability of these polymers to self-assemble into ordered nanostructures, and subsequent lyotropic liquid crystalline properties. The main focus of this report is the direct impact $[Ru(terpy)_2]^{2+}$ complexes have on the polymers' self-assembly in solution and in the bulk. Through this study, answers of some basic questions about organic−inorganic materials were provided. These include the effect of the complex charge on the polymer's ability to have polyelectrolytic properties, the impact these metal complexes have on the polymers' self-assembly in solution and in bulk, the influence of varying the polymers' side chain design, and the combined effect of these various elements on the formation of ordered nanostructures. This initial report begins to set the stage for studying more complex architectures including diblock copolymers where one block contains the metal−ligand complex. Such systems are expected to provide hierarchically ordered materials with two different length scales of organization. At the same time, incorporating metal−ligand chemistries into block copolymer architectures should allow properties of the metal−ligand to be confined to the nanometer length scale. Such materials would be novel, and unexpected properties are likely to follow. Learning to self-assemble macromolecules with the functionality of metal complexes is expected to produce novel advanced materials.

Acknowledgment. We thank the ARO Young Investigator and PECASE programs for generous support of this work. G.N.T. thanks the ONR Young Investigator, NSF-CAREER, 3M Nontenured faculty grant, and Dupont Young Faculty Award programs for support.

Supporting Information Available: Experimental details including synthetic methods, ^1H NMR and ^{13}C NMR spectra, and other experimental findings. This material is available free of charge via the Internet at http://pubs.acs.org.

References and Notes

(1) Ikkala, O.; ten Brinke, G. *Science* **2002**, *295*, 2407−2409.
(2) Stupp, S. *Chem. Rev.* **2005**, *105*, 1023−1024.
(3) Lehn, J.-M. *Supramolecular Chemistry Concepts and Perspectives*; Tokyo, 1995.
(4) Hanabusa, K.; Nakano, K.; Koyama, T.; Shirai, H.; Hojo, N.; Kuroseb, A. *Makromol. Chem.* **1990**, *191*, 391−396.
(5) Hanabusa, K.; Nakamura, A.; Koyama, T.; Shirai, H. *Makromol. Chem.* **1992**, *193*, 1309−1319.
(6) Chujo, Y.; Sada, K.; Saegusa, T. *Macromolecules* **1993**, *26*, 6320−6323.
(7) Chujo, Y.; Sada, K.; Saegusa, T. *Macromolecules* **1993**, *26*, 6315−6319.
(8) Potts, K. T.; Usifert, D. A. *Macromolecules* **1988**, *21*, 1985−1991.
(9) Schmatloch, S.; van den Berg, A. M. J.; Alexeev, A. S.; Hofmeier, H.; Schubert, U. S. *Macromolecules* **2003**, *36*, 9943−9949.
(10) Schmatloch, S.; van den Berg, A. M. J.; Hofmeier, H.; Schubert, U. S. *Des. Monomers Polym.* **2004**, *7*, 191−201.
(11) Dobrawa, R.; Lysetska, M.; Ballester, P.; Grune, M.; Wurthner, F. *Macromolecules* **2005**, *38*, 1315−1325.
(12) Yu, S.-C.; Kwok, C.-C.; Chan, W.-k.; Che, C.-M. *Adv. Mater.* **2003**, *15*, 1643−1647.
(13) Meier, M. A. R.; Wouters, D.; Ott, C.; Guillet, P.; Fustin, C.-A.; Gohy, J.-F.; Schubert, U. S. *Macromolecules* **2006**, *39*, 1569−1576.
(14) Knapton, D.; Rowan, S. J.; Weder, C. *Macromolecules* **2006**, *39*, 651−657.
(15) Knapton, D.; Iyer, P. K.; Rowan, S. J.; Weder, C. *Macromolecules* **2006**, *39*, 4069−4075.
(16) Beck, J. B.; Ineman, J. M.; Rowan, S. J. *Macromolecules* **2005**, *38*, 5060−5068.
(17) Beck, J. B.; Rowan, S. J. *J. Am. Chem. Soc.* **2003**, *125*, 13922−13923.
(18) Hofmeier, H.; Schmatloch, S.; Wouters, D.; Schubert, U. S. *Macromol. Chem. Phys.* **2003**, *204*, 2197−2203.
(19) Tzanetos, N.; Andreopoulou, A. K.; Kallitsis, J. K. *J. Polym. Sci., Part A* **2005**, *43*, 4838−4848.
(20) Hinderberger, D.; Schmelz, O.; Rehahn, M.; Jeschke, G. *Angew. Chem., Int. Ed.* **2004**, *43*, 4616−4621.
(21) Duprez, V.; Biancardo, M.; Spanggaard, H.; Krebs, F. C. *Macromolecules* **2005**, *35*, 10436−10448.
(22) Andreopoulou, A. K.; Kallitsis, J. K. *Eur. J. Org. Chem.* **2005**, 4448−4458.
(23) Zhou, G.; Harruna, I. I. *Macromolecules* **2005**, *38*, 4114−4123.
(24) McAlvin, J. E.; Fraser, C. L. *Macromolecules* **1999**, *32*, 1341−1347.
(25) Johnson, R. M.; Fraser, C. L. *Macromolecules* **2004**, *37*, 2718−2727.
(26) Chen, B.; Sleiman, H. F. *Macromolecules* **2004**, *37*, 5866−5872.
(27) Rezvani, A.; Bazzi, H. S.; Chen, B.; Rakotondradany, F.; Sleiman, H. F. *Inorg. Chem.* **2004**, *43*, 5112−5119.
(28) Pollino, J. M.; Stubbs, L. P.; Weck, M. *Macromolecules* **2003**, *36*, 2230−2234.
(29) Pollino, J. M.; Stubbs, L. P.; Weck, M. *J. Am. Chem. Soc.* **2004**, *126*, 563−567.
(30) Pollino, J. M.; Nair, K. P.; Stubbs, L. P.; Adams, J.; Weck, M. *Tetrahedron* **2004**, *60*, 7205−7215.
(31) Carlise, J. R.; Weck, M. *J. Polym. Sci., Part A* **2004**, *42*, 2973−2984.
(32) Calzia, K. J.; Tew, G. N. *Macromolecules* **2002**, *35*, 6090−6093.
(33) Schubert, U. S.; Hofmeier, H. *Macromol. Rapid Commun.* **2002**, *23*, 561−566.
(34) Gohy, J.-F.; Hofmeier, H.; Alexeev, A.; Schubert, U. S. *Macromol. Chem. Phys.* **2003**, 1524−1530.
(35) Aamer, K. A.; Tew, G. N. *Macromolecules* **2004**, *37*, 1990−1993.
(36) Tew, G. N.; Aamer, K. A.; Shunmugam, R. *Polymer* **2005**, *46*, 8440−8447.
(37) Tew, G. N.; Aamer, K. A.; Shunmugam, R. In *Metal-Containing and Metallosupramolecular Polymers and Materials*; Ulrich, S., Schubert, Newkome, G. R., Manners, I., Eds.; ACS Symposium Series 928; American Chemical Society: Washington, DC, 2006; pp 126−140.
(38) (a) Shunmugam, R.; Tew, G. N. *J. Am. Chem. Soc.* **2005**, *127*, 13567−13572. (b) Shunmugam, R.; Tew, G. N. *J. Polym. Sci., Polym. Chem.* **2005**, *43*, 5831−5843.
(39) Ikkala, O.; Ruokolainen, J.; ten Brinke, G. *Macromolecules* **1995**, *28*, 7088−7094.

(40) Ikkala, O.; Knaapila, M.; Ruokolainen, J.; Torkkeli, M.; Serimaa, R.; Jokela, K.; Horsburgh, L.; Monkman, A.; ten Brinke, G. *Adv. Mater.* **1999**, *11*, 1206−1210.
(41) Ikkala, O.; ten Brinke, G. *Chem. Commun.* **2004**, 2131−2137.
(42) Ruokolainen, J.; ten Brinke, G.; Ikkala, O. *Adv. Mater.* **1999**, *11*, 777−780.
(43) Matyjaszewski, K.; Xia, J. *Chem. Rev.* **2001**, *101*, 2921−2990.
(44) Davis, K. A.; Matyjaszewski, K. *Macromolecules* **2000**, *33*, 4039−4047.
(45) Sauvage, J.-P.; Collin, J.-P.; Chambron, J.-C.; Guillerez, S.; Coudret, C.; Baltani, V.; Barigelletti, F.; Cola, L. D.; Flamigni, L. *Chem. Rev.* **1994**, *94*, 993−1019.
(46) Dobrynin, A. V.; Colby, R. H.; Rubinstein, M. *Macromolecules* **1995**, *28*, 1859−1871.
(47) Russel, W. B.; Saville, D. A.; Schowalter, W. R. *Colloidal Dispersions*; Cambridge University Press: Cambridge, UK, 1989.
(48) Fredrickson, G. H. *Macromolecules* **1993**, *26*, 2825−2831.
(49) Stepanyan, R.; Subbotin, A.; Knaapila, M.; Ikkala, O.; ten Brinke, G. *Macromolecules* **2003**, *36*, 3758−3763.
(50) Khokhlov, A. R.; Semenov, A. N. *J. Stat. Phys.* **1985**, *38*, 161.
(51) Hsieh, H. W. S.; Post, B.; Morawetz, H. *J. Polym. Sci., Polym. Phys. Ed.* **1976**, *14*, 1241−1255.
(52) Antonietti, M.; Burger, C.; Micha, M. A.; Weissenberger, M. *Macromol. Chem. Phys.* **1999**, *200*, 150−155.
(53) Zhao, Y.-F.; Fan, X.-H.; Wan, X.-H.; Chen, X.-F.; Yi, Y.; Wang, L.-S.; Dong, X.; Zhou, Q.-F. *Macromolecules* **2006**, *39*, 948−956.
(54) Cohen, J.; Priel, Z.; Rabin, Y. *J. Chem. Phys.* **1988**, *88*, 7111−7116.
(55) Constable, E. C.; Ward, M. D. *J. Chem. Soc., Dalton Trans.* **1990**, 1405−1409.
(56) Johnson, R. M.; Fraser, C. L. *Biomacromolecules* **2004**, *5*, 580−588.
(57) Dou, S.; Colby, R. H. *Polym. Prepr.* **2004**, *45*, 261−262.

MA062765I